www.nature.com/npp

American College of Neuropsychopharmacology

ARTICLE

Glutamatergic and GABAergic anteroventral BNST projections to PVN CRH neurons regulate maternal separation-induced visceral pain

Si-Ting Huang[1,2,3,5], Ke Wu[1,2,3,5], Miao-Miao Guo[1,2,3], Shuai Shao[1,2,3], Rong Hua[1,2,3,4] and Yong-Mei Zhang[1,2,3]✉

© The Author(s), under exclusive licence to American College of Neuropsychopharmacology 2023

Early-life stress (ELS) is thought to cause the development of visceral pain disorders. While some individuals are vulnerable to visceral pain, others are resilient, but the intrinsic circuit and molecular mechanisms involved remain largely unclear. Herein, we demonstrate that inbred mice subjected to maternal separation (MS) could be separated into susceptible and resilient subpopulations by visceral hypersensitivity evaluation. Through a combination of chemogenetics, optogenetics, fiber photometry, molecular and electrophysiological approaches, we discovered that susceptible mice presented activation of glutamatergic projections or inhibition of GABAergic projections from the anteroventral bed nucleus of the stria terminalis (avBNST) to paraventricular nucleus (PVN) corticotropin-releasing hormone (CRH) neurons. However, resilience develops as a behavioral adaptation partially due to restoration of PVN SK2 channel expression and function. Our findings suggest that PVN CRH neurons are dually regulated by functionally opposing avBNST neurons and that this circuit may be the basis for neurobiological vulnerability to visceral pain.

Neuropsychopharmacology (2023) 48:1778–1788; https://doi.org/10.1038/s41386-023-01678-1

INTRODUCTION

Early-life stress (ELS), such as childhood maltreatment, neglect and separation, not only constitutes a high-risk factor for psychiatric disorders but also relates to the development of chronic visceral pain [1]. However, a growing body of research suggests that some individuals exposed to ELS exhibit resilience to chronic visceral pain [1, 2]. Maternal separation (MS) is a well-characterized paradigm used to study the influence of ELS on brain function and to investigate resilience to psychopathology, but the factors determining susceptibility or resilience to visceral pain have not yet been sufficiently elucidated. Herein, we exploited the large variation in adult outcomes after predictable MS protocol in inbred C57BL/6 mice and investigate the neural circuitry and molecular mechanisms of visceral pain-related behavior.

Visceral hypersensitivity is a multifaceted pathophysiological mechanism underlying the symptoms of viscera- and functional viscera-related pain [3]. Our previous work demonstrated that MS model exhibited visceral hypersensitivity and precipitated pain accompanied by activation of stress-integrative hypophysiotropic corticotropin-releasing hormone (CRH) neurons in the paraventricular nucleus (PVN) of the hypothalamus [4]. CRH neurons receive a diverse array of afferents, including glutamatergic, GABAergic and noradrenergic inputs [5, 6]. The projections that innervate stress-integrative hypophysiotropic CRH neurons mainly originate in local hypothalamic and adjacent forebrain regions. As the "hub" region through which limbic forebrain regions communicate with hypothalamic regions via central visceral circuits [7, 8], the bed nucleus of the stria terminalis (BNST) is undoubtedly the most important nucleus in these circuits.

BNST has attracted attention due to its relevance to pain and psychiatric diseases. Multiple BNST neurocircuitries have been extensively implicated in the regulation of fear, anxiety, depression, addiction, reward, mood and other stress-related disorders [9–13]. Nevertheless, the contribution of neurocircuits involving the BNST, a major relay center of central visceral circuits, to visceral pain has not been well characterized [14]. The latest functional MRI (fMRI) results showed that ELS was associated with lower resting-state-connectivity within the BNST-PVN circuit, which contributes to a dysregulated visceral network response to stress [15]. Sawchenko and Swanson have reported that BNST-innervation of the PVN mostly originate from anteroventral BNST (avBNST) [16]. Consistent with those findings, our research has shown that inhibition of PVN-projecting GABAergic neurons in avBNST contributes to ELS-induced visceral hypersensitivity [17]. The avBNST has long been considered to be densely populated with GABAergic neurons [18], and 1–3% glutamatergic neurons are scattered among these GABAergic cells [19, 20]. However, lesion studies on GABAergic or global avBNST neurons have implied that the impact of the glutamatergic cells outweighs that of the more numerous GABAergic cells, such that the avBNST

[1]NMPA Key Laboratory for Research and Evaluation of Narcotic and Psychotropic Drugs, Xuzhou Medical University, Xuzhou 221004 Jiangsu, China. [2]Jiangsu Province Key Laboratory of Anesthesiology, Xuzhou Medical University, Xuzhou 221004 Jiangsu, China. [3]Jiangsu Province Key Laboratory of Anesthesia and Analgesia Application Technology, Xuzhou Medical University, Xuzhou 221004 Jiangsu, China. [4]Emergency Department, The Affiliated Hospital of Xuzhou Medical University, Xuzhou 221116 Jiangsu, China. [5]These authors contributed equally: Si-Ting Huang, Ke Wu. ✉email: zhangym700@163.com

Received: 9 February 2023 Revised: 11 July 2023 Accepted: 17 July 2023
Published online: 29 July 2023

exerts an overall excitatory influence on the hypothalamic-pituitary-adrenal (HPA) axis [21–24]. Overall, these findings suggest that GABAergic and glutamatergic cells of the avBNST may exert opposite influences on negative emotional states and HPA axis activation.

Therefore, we hypothesized that functionally opposing GABAergic and glutamatergic avBNST projections to PVN CRH neurons might regulate ELS-induced visceral hypersensitivity. In the present study, we combined viral tracing, optogenetics, chemogenetics, fiber photometry, electrophysiology, and visceral hypersensitivity behavior assays to verify the functional organization of the avBNST-PVN pathway and explore the potential molecular mechanisms of susceptibility and resilience to visceral hypersensitivity after MS in mice. This study provides novel information about the avBNST-PVN circuit, which may serve as a therapeutic target for modulating visceral hypersensitivity and pain.

MATERIALS AND METHODS

Experimental animals

C57BL/6 mice were provided by the Experimental Animal Center of Xuzhou Medical University. Neonatal mice generated by mating pairs were reared in standard Plexiglas boxes (290 × 178 × 160 mm) with their mothers until postnatal day 21 (PND21). To avoid the interference of the estrus cycle changes and hormonal disturbances and stress-related susceptibility of females [25, 26], only male offspring were used, and the mice were housed five per cage after weaning and provided *ad libitum* access to chow and water. All animal experiments were performed in accordance with the National Institutes of Health Guide for the Care and Use of Laboratory Animals (NIH Publication No. 8023, revised 1978) and were approved by the Experimental Animal Ethics Committee of Xuzhou Medical University.

MS

A MS model was established according to previous literature reports [4, 27]. The pups were separated from their mothers for 6 h (08:30–11:30 am and 14:30–17:30 pm) each day from PND2 until PND15. During the deprivation episodes, all pups from each litter were removed from their home cage and placed in an incubator maintained at an ambient temperature of 29 ± 1 °C to approximate the warmth of the nest. In addition, cotton and sawdust were provided as bedding so that the pups could thermoregulate as needed. The male pups that did not undergo MS were removed from their cages on PND21, group housed in a new cage and left undisturbed. Other treatments were consistent the MS protocol.

Assessment of visceral pain threshold and abdominal withdrawal reflex (AWR) scores

As described by our previous study [28], mice were fasted but provided *ad libitum* access to water for 18 h before the assessment. A homemade latex balloon (2 cm in length and 1.3–1.5 cm in diameter) was tied to a catheter and connected to a sphygmomanometer and syringe through a three-way pipe. The end of the catheter to which the balloon was tied was inserted into the upper rectum and descending colon, distension was induced and the catheter was withdrawn. AWR scores were assessed at various pressures (20, 40, 60, 80 mmHg), each of which was maintained for 20 s, at an interval of 4 min. The AWR scoring criteria were as follows: 0, no significant behavioral response; 1, immobility or only simple head movement; 2, contraction of abdominal muscles without lifting away from the table; 3, obvious contraction of abdominal wall muscles and lifting away from the table; and 4, abdominal wall arching or bowing of the back and the pelvis. Visible contraction of the abdominal wall, i.e., an AWR score of 3, was considered an indicator of distension pain. The average of at least three scores was calculated for further analysis.

Electromyography (EMG) recording

Mice were fasted but provided *ad libitum* access to water for 18 h before the assessment. The EMG activity of the abdominal external oblique muscle was recorded with a BL-420+ system. The recording parameters were as follows: high frequency filter, 5000 Hz; time constant, 0.01 s; sampling frequency, 1000 Hz; sensitivity, 1 mV; and scanning speed, 250 ms/div.

For the combination of optogenetic manipulation and EMG activity assessment in immobile mice, distension at a pressure of 60 mmHg was used to evoke marked EMG activity. We recorded EMG activity at three points, i.e., before light stimulation, in the presence of light stimulation (10 min) and in the absence of light stimulation (30 min after). EMG activity was recorded during each 8-s distension episode to create a heatmap, with each box representing the peak value for one second.

Brain stereotaxic coordinates

The optimal coordinates of the target nucleus were determined according to Paxinos and Watson brain atlas and were as follows: PVN: AP: −0.94 mm, ML: ±0.25 mm, DV: −5.00 mm; avBNST: AP: 0.14 mm, ML: ±0.75 mm, DV: −4.75 mm.

The mice were anaesthetized with 1% pentobarbital sodium (60 mg/kg, i.p.). The drug or virus suspensions were infused at a rate of 60 nl/min via a microinjection pump, and the needle was kept in place for 10 min to allow full diffuse of the solution. The surgery details and reagents were added to Supplemental Methods. The profiles of reagents and antibodies was shown in supplemental Tables 1, 2. Supplemental Methods also included western blot analysis, immunofluorescence, quantitative real-time PCR, blood sampling and hormone level measurement, and chemogenetic manipulation.

In vitro electrophysiology

In vitro electrophysiology refers to our previous research [28]. Cell-attached recordings of labeled neurons was operated with a borosilicate glass micropipette (BF-150-86-10, Sutter, USA) filled with an internal solution containing (in mM) 10 HEPES, 115 K gluconate, 10 phosphocreatine, 1.5 $MgCl_2$, 2 Mg-ATP, 20 KCl, and 0.5 GTP. While applying the dynamic current clamp, the firing frequency of PVN CRH neurons was recorded under stepped holding current (0–45 pA; Δ = 3 pA). Whole-cell patch-clamp recording of labeled neurons was performed with a patch pipette filled with an internal solution containing (in mM) 5 EGTA, 10 HEPES, 135 K gluconate, 3 Mg-ATP, 0.2 GTP-Na, 0.5 $CaCl_2$, 2 $MgCl_2$ (pH = 7.25, 280–290 mOsm) with an effective resistance of 6–10 MΩ. mEPSCs and mIPSCs were recorded at holding potentials of −60 and −50 mV, respectively. The signals were bandpass filtered at 300 Hz-1 kHz and Bessel filtered at 10 kHz using a Multiclamp700B amplifier. Data acquisition and analysis were conducted with Clampex and Clampfit 10 software (Axon Instruments).

Optogenetic manipulation

For optogenetic manipulation in mice, an optical fiber was implanted 200 μm above the third ventricle, which is adjacent to the PVN (from bregma: AP: −0.94 mm, ML: ±0.25 mm, DV: −4.80 mm). For ChR2-mediated photoactivation, 473-nm laser pulses (10 Hz, 10-ms pulse-width) (BL473T3-100FC, Lasercentury, China) were delivered for 5–10 min. For NpHR-mediated photoinhibition, 589-nm laser pulses (duration of 8 s, interval of 2 s) (YL589T6-100FC, Lasercentury, China) were utilized for 5–10 min. The optical power was 1.8 mW for the blue laser (473 nm) and 3.5 mW for the yellow laser (589 nm), as measured at the tip of the optic fiber.

For intracerebral drug administration in the optogenetic experiments, a fiber optic cannula (RWD) was implanted above the PVN (from bregma: AP: −0.94 mm, ML: ±0.25 mm, DV: −4.80 mm). Except for L-Glu, which was administrated 1 h before optogenetic stimulation, all pharmacological intervention was performed 30 min before optogenetic experiment.

Statistics and analysis

All data are expressed as the mean ± SEM. Differences between two groups were evaluated by independent sample Student's *t* test, and those among multiple groups were analyzed by one-way ANOVA or two-way repeated measures ANOVA. If a significant difference was found, Bonferroni or Tukey's multiple comparisons *post hoc* test was performed. Data analysis were contacted with SPSS 16.0 (IBM, Armonk, NY) software package. Figures were generated and analyses were performed in GraphPad Prism 7.0 (Graph Pad Software). $*p < 0.05$ was considered statistically significant.

RESULTS

Separation of MS mice into visceral hypersensitivity-susceptible and visceral hypersensitivity-resilient populations

To determine the difference in visceral nociceptive sensitization in adult mice subjected to neonatal MS, we meased a series of

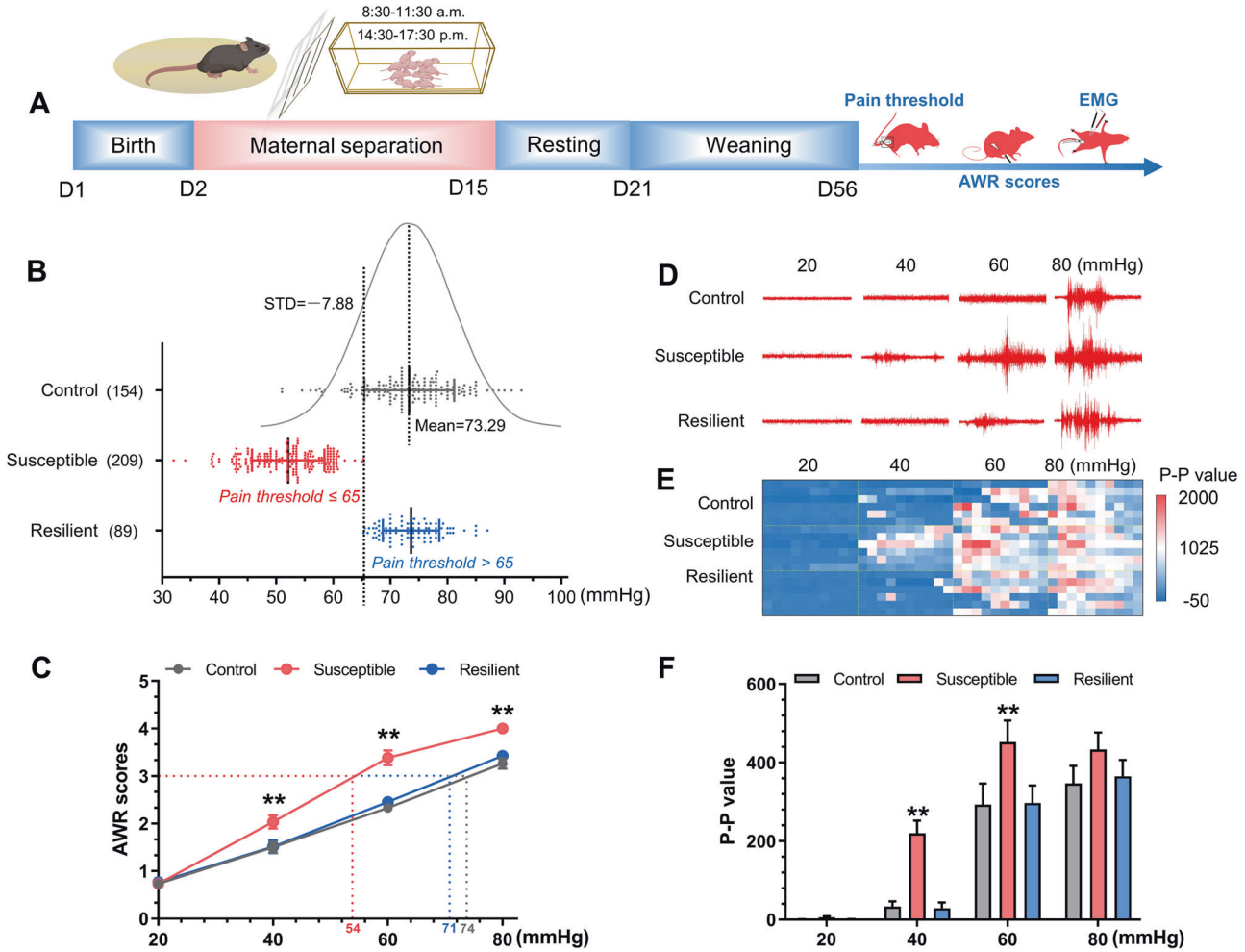

Fig. 1 Separation of mice exposed to MS into susceptible and unsusceptible populations. A Schematic diagram of the neonatal MS protocol and related behaviors in adulthood. **B** The visceral pain threshold was significantly decreased in susceptible mice compared with control and unsusceptible mice ($n = 10$). **C** The AWR score was significantly increased in susceptible mice compared with control and unsusceptible mice during CRD at pressures of 20, 40, 60 and 80 mmHg ($n = 10$). **D**, **E** The EMG activity of the external oblique muscle and the associated heatmap are shown ($n = 6$). **F** Susceptible mice presented an increase in activity in response to CRD at 40, 60 and 80 mmHg. The data are expressed as the mean ± SEM. $^{**}p < 0.01$.

visceral receptivity indicators in the mice. A schematic diagram of the neonatal MS protocol and related behaviors in adulthood is shown in Fig. 1A. We used the performance of the non-MS group to represent the behavior of the normal population and characterized the distribution of pain threshold values in the control group. Standard deviations were utilized to calculate the lower and upper "cut-off values" for the visceral pain threshold. Then, the pain threshold value of the MS group was compared to the distribution curve of the control group. The mean ± SD of the visceral pain threshold evaluated by colorectal distension (CRD) was 73.29 ± 7.88. Therefore, the lower "cut-off value" was set to 65 mmHg: mice with a pain threshold ≤65 mmHg were labeled "susceptible", and those with a pain threshold >65 mmHg were labeled "resilient" (Fig. 1B). We found that approximately 30% of mice in the MS group displayed visceral responses similar to those of mice in the non-MS group.

Further analyses supported the authenticity of the differences between the susceptible and resilient phenotypes. The AWR scores of the susceptible mice were significantly higher than those of the control and resilient mice (Fig. 1C). The electromyographic (EMG) activity of the external oblique muscle is a classical objective index of visceral sensitization; EMG activity and the associated heatmap are shown (Fig. 1D, E). We observed an increase in EMG activity in response to graded colorectal distention (CRD) in susceptible mice (Fig. 1F). These results implied that susceptible mice exhibited more severe stress responses when subjected to CRD. However, resilient mice seemed to adapt well in response to adverse conditions. The scientific consensus is that hormones are not a valid excuse to exclude female mice from studies. Thus, we added behavioral data for female mice (Supplementary Fig. 1). The normal female mice showed similar basal visceral pain thresholds compared with the male group (73.68 ± 9.15 vs. 73.29 ± 7.88). When the "cut-off behavioral criteria" analysis method used to distinguish male mice was applied to female mice, we found that more than 70% of predictable MS female mice showed visceral hypersensitivity resilience, and the percentage of resilience will further increase as the sample size increases.

Activation of CRH neurons within the PVN mediates susceptibility rather than resilience to visceral hypersensitivity

To examine the differential responses of CRH neurons to ELS-induced visceral hypersensitivity, we evaluated the expression and activation of CRH neurons in the PVN. RT-PCR demonstrated that CRH gene expression in the PVN in susceptible mice was

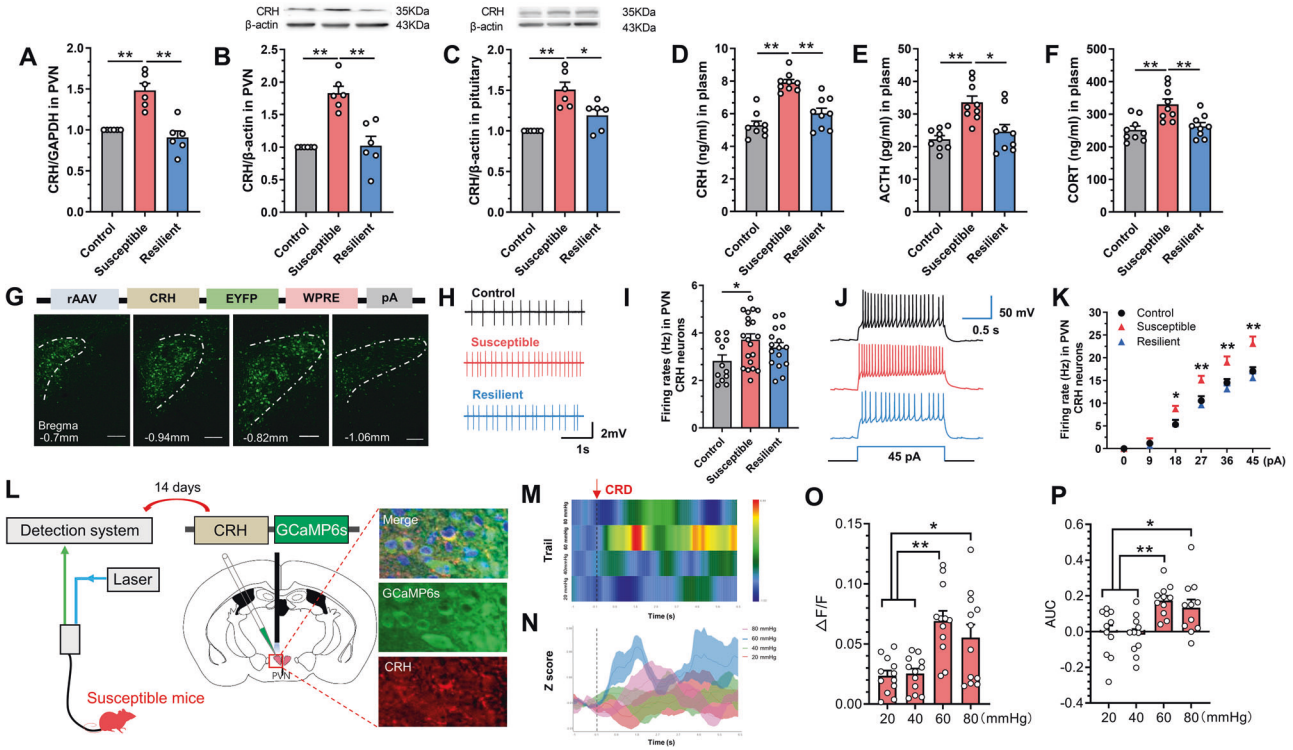

Fig. 2 Activation of CRH neurons within the PVN mediates susceptibility. A RT-PCR demonstrated that CRH gene expression in the PVN of susceptible mice was significantly higher than in the PVN of control and unsusceptible mice ($n = 6$). **B** Western blot analysis revealed that CRH protein expression in the PVN was significantly elevated in susceptible mice ($n = 6$). **C** CRH protein expression in pituitary tissues was significantly increased ($n = 6$). **D**–**F** The serum levels of CRH, ACTH, and CORT were significantly increased in susceptible mice compared with control and resilient mice ($n = 9$). **G** The mapping of PVN by a CRH-specific promoter virus. Scale bar = 100 μm. **H**–**I** The spontaneous firing frequency of susceptible mice was significantly increased compared with that of control and resilient mice ($n = 12$–20 discharges from 6 mice). **J** Schematic diagram of the evoked firing rate in response to a stepwise increase in stimulus intensity in the three groups. **K** Susceptible mice presented an increased firing in response to the stimulus intensity at 18, 27, 36, 45 pA. **L** Experimental approach for GCaMP6s signal recordings. Heat map (**M**) and Z score (**N**) schematic diagram. Average GCaMP6s responses (**O**) and quantification of the area under the curve (AUC) (**P**) showed that the GCaMP6s signal in the PVN CRH neurons of susceptible mice was significantly increased following 60 and 80 mmHg CRD. The data are expressed as the mean ± SEM. *$p < 0.05$, **$p < 0.01$.

significantly higher than that in control and resilient mice (Fig. 2A). Western blot analysis of PVN and pituitary tissues revealed that CRH protein expression was significantly elevated in susceptible mice (Fig. 2B, C). In addition, immunofluorescence showed that the number of c-Fos-positive CRH neurons in the PVN was significantly higher in the susceptible group than in the control and resilient groups (Supplementary Fig. 2A, B). Furthermore, the HPA axis was significantly activated in the susceptible group compared with the control and resilient groups (Fig. 2D–F). The serum levels of CRH, ACTH, and CORT were significantly increased in susceptible mice compared with control and resilient mice (Fig. 2D–F). Next, we tested the activity of CRH neurons in the PVN by ex vivo electrophysiological recordings. The PVN was delineated in four planes by a CRH-specific promoter virus (Fig. 2G). The efficiency of the virus was verified by an anti-CRH antibody (Supplementary Fig. 2C). The percentage of neurons positive for both anti-CRH- and rAAV-CRH-positive neurons was 99.1% (Supplementary Fig. 2D). Patched PVN CRH neurons were recorded, and the recordings are shown in Supplementary Fig. 2E. As expected, the spontaneous firing frequency of CRH neurons in the PVN (Fig. 2H, I) and the evoked firing rate in response to a stepwise increase in stimulus intensity (18–45 pA) (Fig. 2J, K) were significantly elevated in susceptible mice compared with control and resilient mice.

Next, to quantify the physiological activity of PVN CRH neurons during visceral stimuli behaviors, we infused a Cre-dependent adeno-associated virus (AAV) expressing a Ca2+-sensor protein (GCaMP6s) in PVN CRH neurons in susceptible and measured GCaMP6s fluorescence changes (Fig. 2L). Schematic diagram of heat map (Fig. 2M) and Z score (Fig. 2N) was shown. In vivo fiber photometry recordings revealed that the GCaMP6s signal in the PVN CRH neuron of susceptible mice was significantly increased following 60 and 80 mmHg CRD (Fig. 2O, P). Together, these results suggest that the activity of CRH neurons in the PVN does not change uniformly in response to visceral stimuli and can be used to distinguish susceptibility and resilience following MS.

An imbalance between excitatory and inhibitory avBNST inputs to PVN CRH neurons facilitates visceral hypersensitivity in susceptible mice

To test whether presynaptic changes in excitatory or inhibitory afferents alter the excitability of PVN CRH neurons, we selectively transduced CRH neurons in the PVN with a recombinant adeno-associated virus (rAAV) to label these neurons. The efficiency of rAAV transduction has been demonstrated previously [17], miniature excitatory postsynaptic current (mEPSCs) and miniature inhibitory postsynaptic current (mIPSCs) were recorded in major parvocellular CRH neurons adjacent to the third ventricle. We found that the firing frequency of mEPSCs in the susceptible group was markedly elevated compared with that in the control and resilient groups, suggesting that CRH neurons received massive excitatory extrasynaptic inputs (Fig. 3A, B). The amplitude of mEPSCs was increased in susceptible compared with naïve mice (Fig. 3C), indicating the enhancement of excitatory synaptic efficiency, more intriguingly, resilient mice also presented increasing excitatory synaptic efficiency. Compared with control

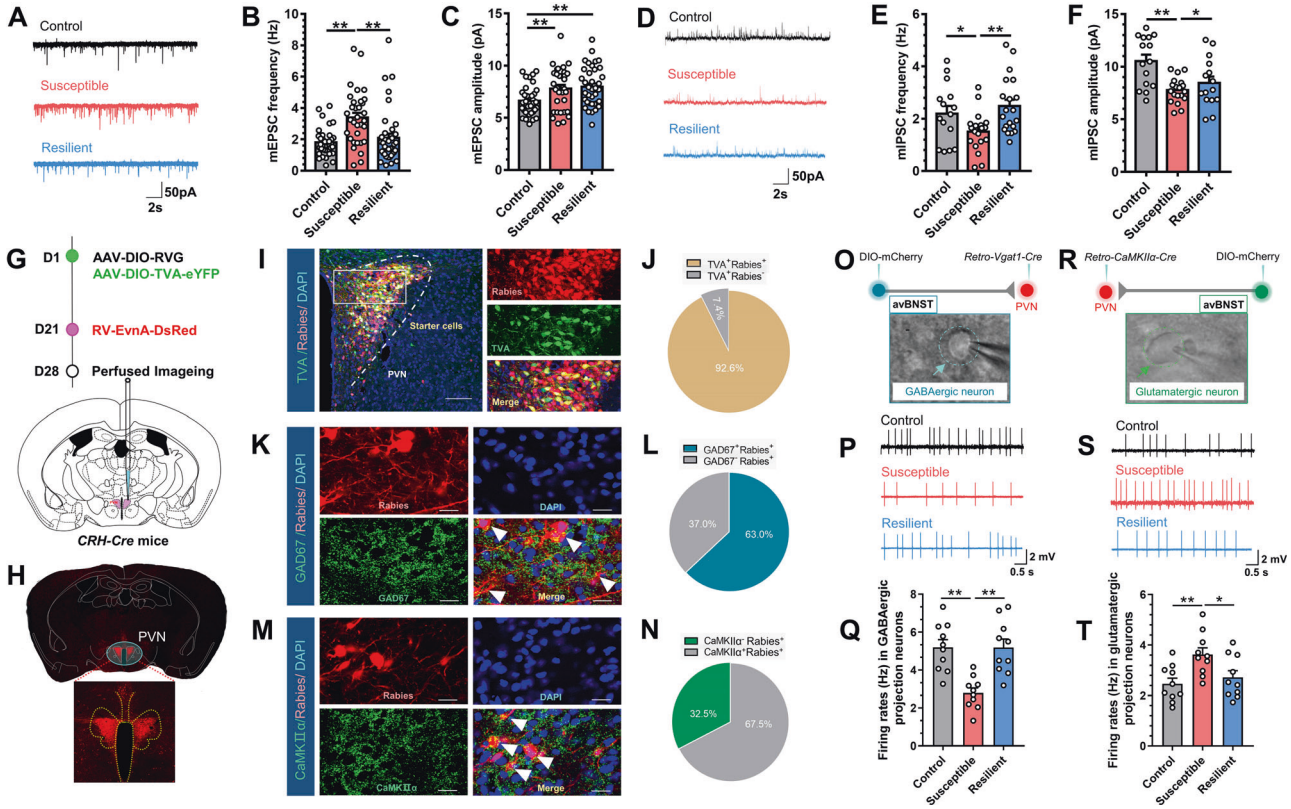

Fig. 3 Mapping of the connections between glutamatergic and GABAergic avBNST neurons and PVN CRH neurons. **A** Representative traces of mEPSCs in PVN CRH neurons (n = from 6 mice). **B** The mEPSC frequency in parvocellular CRH neurons was significantly increased in brain slices from susceptible mice compared with those from control and resilient mice (n = from 6 mice). **C** The mEPSC amplitude in PVN CRH neurons was significantly increased in susceptible and resilient mice compared with control mice (n = from 6 mice). **D** Representative traces of mIPSCs in PVN CRH neurons (n = from 6 mice). The mIPSC frequency (**E**) and mIPSC amplitude (**F**) in parvocellular CRH neurons was significantly decreased in brain slices from susceptible mice compared with those from control and resilient mice (n = from 6 mice). **G** Schematic showing injection of AAV-Ef1α-DIO-TVA-eGFP and AAV-Ef1α-DIO-RVG into the PVN on day 1 and RV-EvnA-DsRed into the PVN on day 21 in CRH-Cre mice. **H** The mapping of PVN by Rabies-DsRed signal. **I** The Rabies-DsRed signal was colocalized with TVA immunofluorescence in the PVN. **J** The percentage of cells positive for both TVA and RV in the PVN was 92.6% (n = 3). **K** Representative images of DsRed and GAD67 in the avBNST. Scale bar = 20 μm. **L** The percentage of cells positive for both RV and GAD67+ in the avBNST was 63.0% (n = 3). **M** Representative images of DsRed and CamKIIα expression in the avBNST. Scale bar = 20 μm. **N** The percentage of cells positive for both of RV and CamKIIα+ in the avBNST was 32.5% (n = 3). Patched PVN-innervating avBNST GABAergic (**O**) and glutamatergic (**R**) neurons were recorded. **P**, **S** Schematic diagrams of spontaneous firing frequency in the three groups were shown. The firing rate of PVN-innervating avBNST GABAergic (**Q**) and glutamatergic (**T**) neurons was decreased and increased respectively in susceptible mice compared with those from control and resilient mice (n = from 5 mice). The data are expressed as the mean ± SEM. *$p < 0.05$, **$p < 0.01$.

and resilient mice, susceptible mice presented significant decreases in mIPSC firing frequency and amplitude (Fig. 3D–F), indicating a reduction in inhibitory extrasynaptic inputs and postsynaptic efficiency in CRH neurons in the PVN in susceptible mice. These results indicate that the balance between excitatory and inhibitory synaptic inputs is altered in susceptible mice, resulting in excitation of PVN CRH neurons. Nevertheless, in resilience mice, the balance between excitatory and inhibitory synaptic inputs innervating PVN CRH neurons was relatively maintained in addition to the increased excitatory postsynaptic efficiency, indicating there were compensatory changes in CRH neurons rather than neural circuits. So, what mechanism account for the compensatory of excitatory postsynaptic efficiency? These disparities likely due to the different expression and function of one or more intrinsic voltage-gated or voltage-independent currents in PVN CRH neurons. Thus, we mainly investigated the neural circuitry involved in visceral hypersensitivity susceptibility and then focused on the intrinsic ion channels activity of CRH neurons in resilient mice.

Next, we transduced CRH neurons in the PVN with a modified rabies virus (RV) (cell-type-specific retrograde trans-monosynaptic tracing system) to identify the upstream targets of these CRH neurons. At least 3 weeks after unilateral injection of Cre-dependent helper viruses (AAV-EF1α-DIO-TVA-eYFP and AAV-EF1α-DIO-RVG) into the PVN to induce the expression of RVG in CRH-Cre mice, RV (EnvA-pseudotyped RV-ΔG-DsRed) was injected into the same site (Fig. 3G). Retrograde RV spreads by means of helper viruses [29]. The initial expression of RV was shown (Fig. 3H). We found that DsRed-labeled neurons were robustly distributed in many emotion-related nuclei, including the avBNST, nucleus accumbens (NAc), medial preoptic area (MPA), anterior hypothalamic area, posterior part (AHP), lateral sulcus (LS), medial prefrontal cortex (mPFC), zona inerta (ZI), dorsomedial hypothalamic nucleus (DM), ventromedial hypothalamus (VMH), arcuate nucleus (Arc), ventral tegmental area (VTA), and so on (Supplementary Fig. 3A, B). To investigate the functions of these potential upstream targets in visceral hypersensitivity is our main objective.

Considering that avBNST possessed the most two cell types, we need to distinguish the role of GABAergic and glutamatergic avBNST-PVN neurons in the following experiments. First of all, the morphological properties of avBNST-PVN circuits were examined. Representative images of starter cells from the PVN of CRH-Cre mice are shown in Fig. 3I. The efficiency of the TVA+RV+ retrograde tracing was approximately 92.6% (Fig. 3J). We further

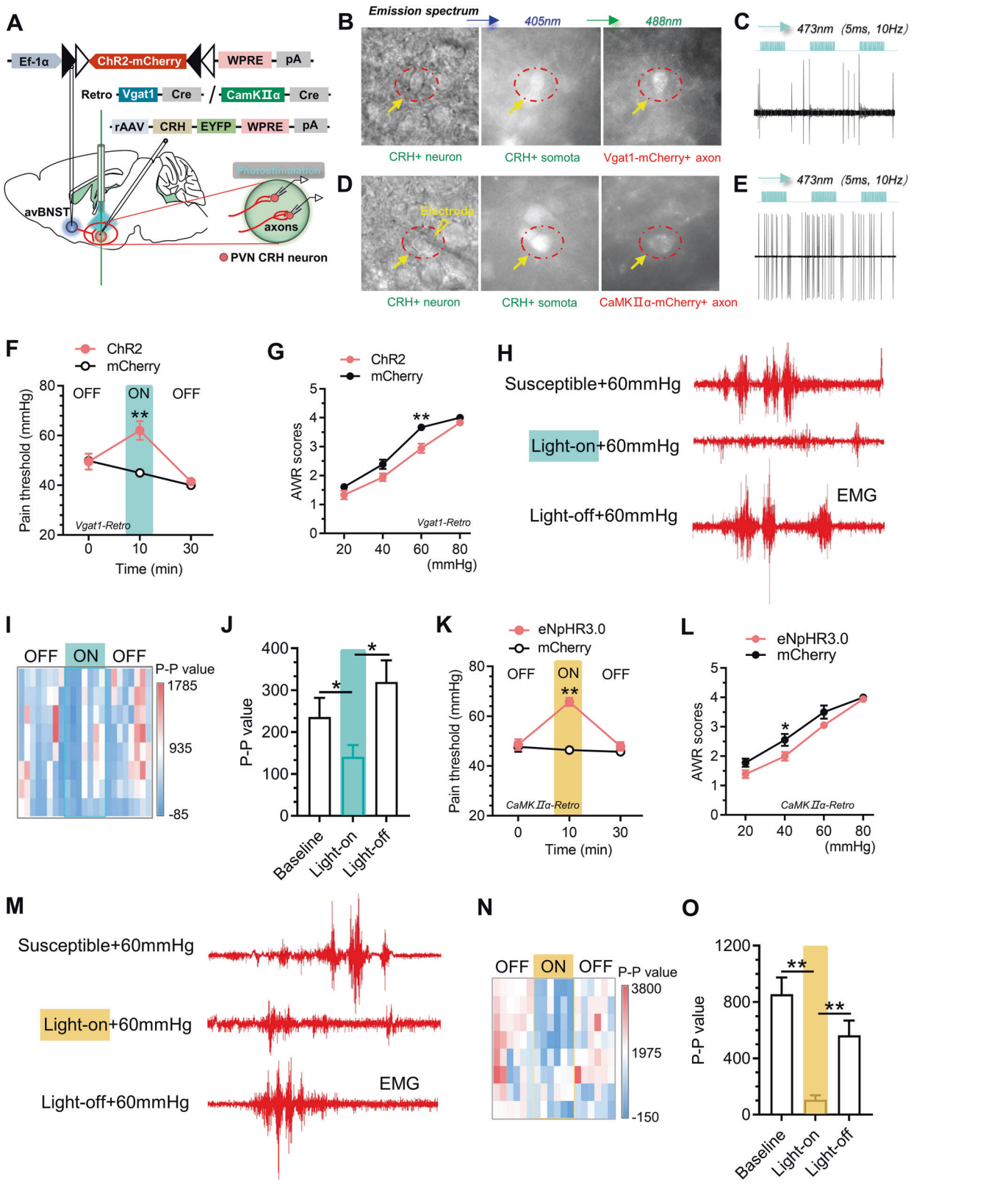

studied GABAergic avBNST inputs to PVN CRH neurons and found that a majority of avBNST neurons sent dense GABAergic afferents (63.0%) to innervate CRH neurons within the PVN (Fig. 3K, L). Moreover, we identified the GABAergic subtypes of avBNST-PVN projecting neurons by GABA antibody staining. The Vgat1-positive neurons in avBNST can be stained well with anti-GABA antibody (Supplementary Fig. 4A, B). In addition, 32.5% of projecting neurons in the avBNST were glutamatergic cells (Fig. 3M, N).

We subsequently aimed to identify the excitability of PVN-innervating glutamatergic and GABAergic avBNST neurons in

Fig. 4 Identification of the functional connections in the GABAergic/glutamatergic avBNST-PVN CRH neuron pathway and the effect of optogenetic modulation of this pathway on behavior. A Experimental scheme used to assess the functional connection of GABAergic/glutamatergic avBNST-PVN CRH neuron projections. **B**, **D** Representative images of presynaptic inputs to PVN CRH neurons. **C**, **E** Schematic diagram of CRH neuron activity following blue light stimulation. (**F**) The visceral pain threshold was significantly increased after activation of the GABAergic avBNST-PVN circuit in susceptible mice, and the AWR score was decreased (**G**). **H**–**J** The peak-to-peak value of external oblique muscle activity was decreased under blue light stimulation in susceptible mice expressing Vgat1-ChR2 compared with vehicle-treated mice group. **K**, **L** The visceral pain threshold was significantly increased and the AWR score was decreased after inhibition of the glutamatergic avBNST-PVN circuit. **M**–**O** The peak-to-peak value of external oblique muscle activity was decreased upon yellow light stimulation in susceptible mice expressing CaMKIIα-eNpHR3.0 compared with vehicle-treated mice. The data are expressed as the mean ± SEM. $*p < 0.05$, $**p < 0.01$.

mice. Retrogade virus rAAV-Vgat1-Cre-WPRE-PA was injected into PVN, and rAAV-Ef1α-DIO-mCherry was injected into avBNST. 21 days later, the patched PVN-innervating avBNST neurons were recorded (Fig. 3O, R). A schematic diagram of spontaneous firing frequency in the three groups is shown (Fig. 3P, S). Compared with control and resilient mice, susceptible mice presented significant decreases firing rates in PVN-innervating GABAergic avBNST neurons (Fig. 3Q), and increased firing rates in PVN-innervating glutamatergic avBNST neurons (Fig. 3T). These results demonstrated that the inhibitory projection neurons from avBNST to PVN was decreased and the excitatory projection neurons was increased in susceptible mice.

Photomanipulation of glutamatergic and GABAergic avBNST projections to PVN CRH neurons regulates visceral hypersensitivity in susceptible mice

In the sections above, neurotransmission was assessed by studying avBNST neurons projecting to PVN CRH neurons. Next, we examined whether avBNST neurons contribute to the regulation of ELS-induced visceral hypersensitivity.

Chemogenetic activation of GABAergic neurons or inhibition of glutamatergic neurons in the avBNST-PVN circuit alleviates visceral hypersensitivity in susceptible mice (Supplementary Fig. 5).

To address the functional properties of GABAergic and glutamatergic avBNST neurons projecting to PVN CRH neurons, we performed an ex vivo acute brain slice preparation method that allowed us to preserve PVN neurons and obtained cell-attached recordings from anterogradely colabelled CRH neurons. A schematic diagram of the stereotaxic AAV injection protocol is shown in Fig. 4A. ChR2-mCherry fluorescence was observed in the soma of avBNST neurons surrounding PVN CRH-EYFP neurons, confirming that the neurons that extended ChR2-mCherry-expressing axons were GABAergic and glutamatergic avBNST neurons (Fig. 4B, D). We administered blue light pulses and observed that spontaneous firing of PVN CRH neurons was abolished after activation of inhibitory GABAergic synaptic inputs from the avBNST. Moreover, the light-induced changes in CRH neuron firing were reversed after the cessation of light stimulation (Fig. 4C). In contrast, firing frequency was significantly elevated after activation excitatory glutamatergic synaptic inputs from the avBNST (Fig. 4E). These results showed that GABAergic and glutamatergic avBNST neurons form functional synapses with PVN CRH neurons.

Next, we assessed whether photomanipulation of avBNST-PVN circuits in vivo alters nociceptive visceral pain. A schematic of the protocol used for virus administration and cannula implantation in susceptible mice is shown (Supplementary Fig. 6A). ChR2-mCherry-expressing GABAergic avBNST cells were labeled with an anti-GAD67 antibody (Supplementary Fig. 6B). Blue light was delivered into the PVN, and we found that optic stimulation of GABAergic avBNST afferents increased the visceral pain threshold in susceptible mice (Fig. 4F) and decreased the AWR score (Fig. 4G). Then, we measured the activity of the external oblique muscle upon manipulation of the GABAergic avBNST-PVN circuit. A schematic diagram showing EMG activity is shown in Fig. 4H. A heatmap showing external oblique muscle EMG activity is shown in Fig. 4I. The peak-to-peak value of external oblique muscle EMG activity was significantly decreased in susceptible mice under blue light administration (Fig. 4J). Next, we manipulated glutamatergic avBNST-PVN circuits by selectively inhibiting glutamatergic avBNST terminals in the PVN of susceptible mice. As expected, yellow light administration elevated the visceral pain threshold (Fig. 4K), decreased the AWR score (Fig. 4L) and reduced external oblique muscle EMG activity (Fig. 4M–O). The corresponding photogenetic stimulation experiments were attached in Supplementary Fig. 6C–G. Together, these results suggested that GABAergic and glutamatergic avBNST-PVN circuits collaboratively regulate visceral hypersensitivity following neonatal MS.

Ion channels are membrane proteins, which play a principal role in modulating cellular excitability. In the ion channels of glutamatergic synaptic transmission, NMDA receptors (NMDARs) play a crucial role in physiological synaptic functions, and the current recorded by patch-clamp electrophysiological technique primarily derived of AMPAR. Moreover, GABAA receptors (GABAARs) are ligand-gated ion channels involved in synaptic transmission of GABAergic neurons. To further investigate the molecular mechanisms involved in avBNST-PVN circuits, we tested the effects of AMPA receptors (AMPARs) and GABAARs in PVN CRH neurons in susceptible mice in vivo (Supplementary Fig. 7A–K). We found that GABAARs and AMPARs in GABAergic and glutamatergic avBNST-PVN circuits mediate visceral hypersensitivity in susceptible mice. These results provide strong evidence for the potential molecular mechanisms involved in avBNST-PVN circuits.

In addition, we also assessed the role of VMH-PVN and NAc-PVN neurocircuitry in visceral hypersensitivity (Supplementary Fig. 8A–C). We observed yellow photo-inhibition of the VMH/NAc terminals in the PVN had no effect on the visceral hypersensitivity in susceptible group.

SK2 expression and activity rescue visceral hypersensitivity in resilient mice

As mentioned in Fig. 3C, excitatory postsynaptic efficiency was also increased in resilient mice, which was inconsistent with its behavioral results. We hypothesized that these disparities maybe due to the compensatory strategy of intrinsic ion channels of PVN CRH neurons. As well known, hyperpolarization is a phase which contributes to reduce the intrinsic excitability and synaptic transmission of neurons. SK2 channels, voltage-independent, Ca^{2+}-activated ion channels, are involved in the postspike hyperpolarization in PVN in visceral hypersensitivity [30]. However, the mechanisms underlying the effects of SK2 on PVN CRH neurons are currently unclear. Finally, we examined the expression and function of SK2 channels, confirming the rescue role of SK2 in visceral hypersensitivity resilient mice.

Western blot analysis of PVN tissues revealed that membrane SK2 protein expression was significantly elevated in resilient mice (Fig. 5A). Representative images of PVN cells expressing the SK2 protein are shown (Fig. 5B). Morphological analysis suggested that SK2 expression in susceptible mice was significantly decreased compared with that in control and resilient mice (Fig. 5C). Herein, we observed an increase in afterhyperpolarization currents (I_{AHP}) of SK2 channels in resilient mice (Fig. 5D, E). We then assessed

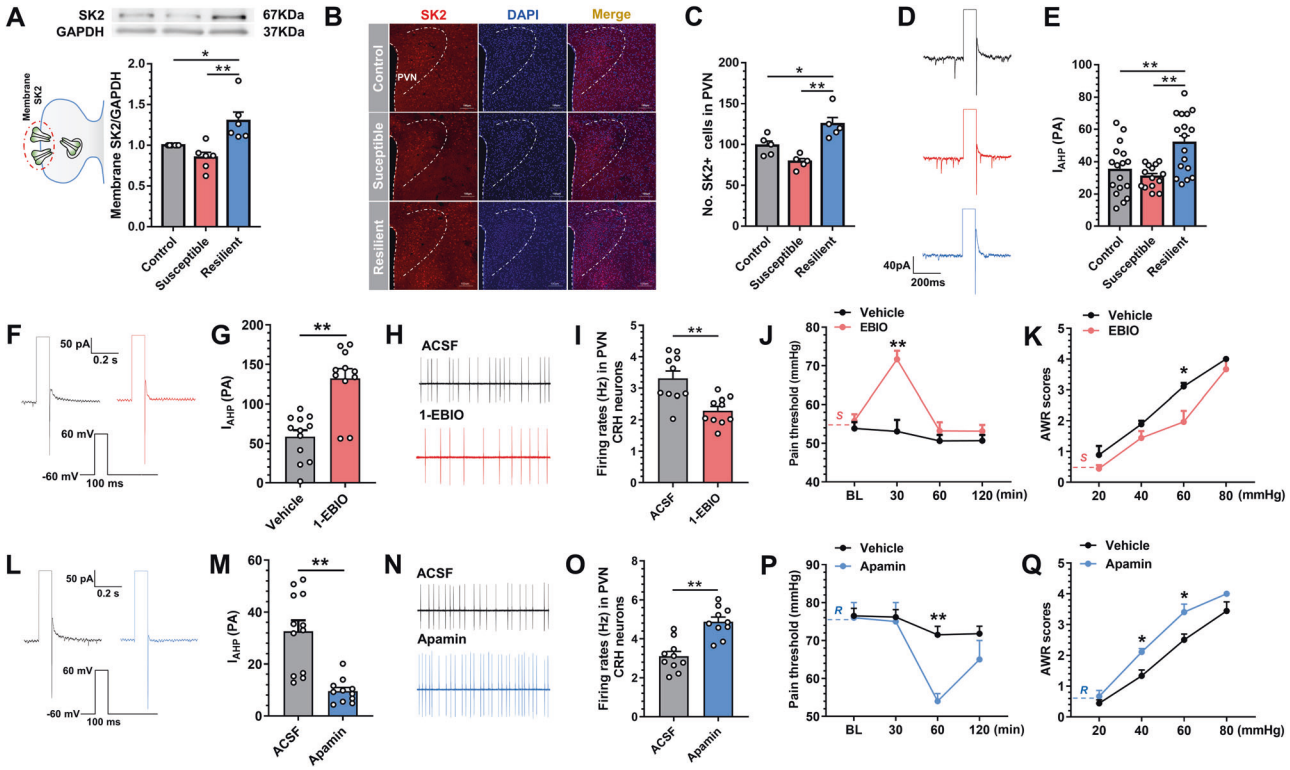

Fig. 5 Restoring SK2 expression and function in resilient mice rescues visceral hypersensitivity. A SK2 protein expression in the PVN was significantly increased in resilient mice compared with control and susceptible mice. **B** SK2 channel immunostaining. Scale bar = 100 μm. **C** The number of SK2 channels in the PVN was increased in resilient mice compared with control and susceptible mice. **D**, **E** The I_{AHP} of CRH neurons in the PVN in resilient mice was significantly increased compared with that in control and susceptible mice. **F**, **G** 1-EBIO administration increased the I_{AHP} amplitude in naïve mice. **H**, **I** 1-EBIO administration decreased the firing rate of CRH neurons in the PVN. **J** The visceral pain threshold was significantly elevated 30 min after 1-EBIO treatment in susceptible mice. **K** The AWR score was significantly decreased after 1-EBIO treatment in susceptible mice subjected to stimulation at a pressure of 60 mmHg. **L**, **M** Compared with DMSO injection, apamin injection decreased the I_{AHP} amplitude in naïve mice. **N**, **O** Compared with DMSO injection, apamin injection increased the firing rate of CRH neurons in the PVN. **P** The visceral pain threshold was significantly decreased in apamin-treated resilient mice compared with vehicle-treated mice 1 h after drug administration. **Q** The AWR score was significantly increased after apamin administration in resilient mice subjected to stimulation at pressures of 40 mmHg and 60 mmHg. The data are expressed as the mean ± SEM. $^{*}p < 0.05$, $^{**}p < 0.01$.

whether promotion of SK2 function rescues inhibitory currents in PVN CRH neurons in slices from susceptible mice slices. The evoked inhibitory current amplitude was significantly larger in slices from 1-EBIO-treated mice than in slices from vehicle control mice (Fig. 5F, G). Moreover, cell-attached recordings revealed that the spontaneous firing rate of CRH neurons in the PVN was decreased after 1-EBIO perfusion (Fig. 5H, I). Accordingly, administration of 1-EBIO into the PVN increased the visceral pain threshold and decreased the AWR score in susceptible mice (Fig. 5J, K). Similarly, the evoked inhibitory current amplitude was significantly reduced in apamin-treated slices compared to vehicle controls (Fig. 5L, M). Cell-attached recordings showed that the spontaneous firing rate of CRH neurons in the PVN was increased after apamin perfusion (Fig. 5N, O). The visceral pain threshold was reduced and the AWR score was elevated in resilient mice administered apamin into the PVN compared with vehicle control mice (Fig. 5P, Q). This finding implied that restored SK2 expression and function is essential to desensitize PVN CRH neurons in resilient mice, but the mechanisms underlying the restoration of SK2 channels still need to be elucidated.

DISCUSSION

Gastrointestinal responses to ELS tend to be variable, with some individuals exhibiting resilience. Here, we adopted an MS paradigm and separated mice into two subgroups according to their visceral hypersensitivity. Stimulated the glutamatergic avBNST-PVN CRH neuron pathway and inhibited GABAergic avBNST-PVN CRH neuron pathway, which activated PVN CRH neurons and subsequently the HPA axis, promoting susceptibility to visceral hypersensitivity in mice exposed to MS. AMPARs and GABAARs played vital roles in regulating neuronal excitability and synaptic transmission in response to glutamate and GABA, respectively, in the avBNST-PVN pathway. In contrast, the relative balance of excitatory/inhibitory synaptic transmission via the avBNST-PVN pathway and the restoration of SK2 channels, which contribute to the recovery of intrinsic excitability of PVN CRH neurons, give rise to resilience to visceral hypersensitivity in mice exposed to similar adverse conditions.

MS may permanently influence an individual's vulnerability or resilience to stress-related disorders later in life. In rodents, this discrepancy is likely due to variations in the species of animals used or the MS protocol [31], including the time, duration, and predictability of MS and the sex, which have a critical effect on phenotype. Actually, the females seem to be more susceptible to the negative effects of ELS, which contribute to the female predominance of chronic visceral hypersensitivity in clinical populations [32, 33]. However, it has been shown that in female rats, unpredictable ELS confers susceptibility and results in visceral hypersensitivity, whereas predictable ELS induces resilience in adulthood without causing visceral hypersensitivity. Additionally, this resilience is lost after exposure to chronic stress in adulthood leading to an intensification of visceral hypersensitivity [34–36]. In our paradigm, most of predictable MS females displayed visceral

hypersensitivity resilience in adulthood. It is also possible that current visceral pain measurements are relatively insensitive to female mice, and we believe that the differences between susceptibility and resilience in female mice will be elucidated in future experiments with advances in the detection of visceral pain.

In this study, we systematically demonstrated that MS is associated with distinct phenotypes of susceptibility and resilience to visceral hypersensitivity in adults. While studies have overlooked inhibition of the HPA axis in response to MS, most studies have demonstrated that CRH neurons and the HPA axis partly account for the high comorbidity between functional visceral pain and psychiatric conditions [37], which is coincident with our findings in visceral hypersensitivity susceptible mice. Our fiber photometry data showed that the activation of PVN CRH neurons was enhanced in susceptible mice in response to gradient CRD (Fig. 2O, P). Furthermore, PVN CRH neurons were hyperactive in the visceral hypersensitivity state, as evidenced by increased c-Fos expression (Supplementary Fig. S1A, B) and firing frequency (Fig. 2H–K). Whole-cell patch-clamp recording of PVN CRH neurons showed significant increases in mEPSC firing frequency/amplitude and decreases in mIPSC firing frequency/amplitude in susceptible mice (Fig. 3A–F). Previous reports have shown that increased glutamatergic transmission through synapses on CRH-releasing neurons in the PVN is a common maladaptation to ELS [38]. It has also been proposed that inadequate GABAergic inhibition increases the activity of CRH neurons and subsequently activates the HPA axis [39]. We further clarified that PVN CRH neurons received direct long-range inputs from multiple brain regions, such as the avBNST, the dorsomedial part of the ventromedial hypothalamus (VMHDM), ventrolateral part of the ventromedial hypothalamus (VMHVL), MPA, Arc, NAc, VTA, AHP, LS and mPFC (Supplementary Fig. S2A, B).

Longitudinal studies assessing the relationship between ELS and visceral neural circuits formed by the PVN, BNST, amygdala and subgenual anterior cingulate cortex have revealed neurobiological vulnerability to poor health outcomes [7]. Notably, ELS in the form of MS renders individuals vulnerable to behavioral deficits, potentially due to dysfunction and incomplete development of the PVN and BNST during early postnatal life [40]. Our previous studies demonstrated that inhibition of the GABAergic avBNST-PVN circuit participated in the occurrence of visceral hypersensitivity in neonatal MS- or CRD-induced ELS models [17, 28]. Herein, we further clarified that glutamatergic avBNST neurons differentially regulate susceptibility to visceral hypersensitivity. Usually, glutamatergic and GABAergic neurons in the ventral BNST differ in their physiological properties and exert functionally opposing effects in neural circuits to regulate emotion and motivation [41, 42]. Our findings indicate that the avBNST contains divergent functional neurons that play different roles in response to MS induced visceral hypersensitivity, and further suggest that excitatory as well as inhibitory limbic information is funneled through PVN CRH neurons. By what molecular mechanism do avBNST-PVN neural circuits affect PVN CRH neurons?

Ion channels are an important molecular mechanism serving as the principal integrating and modulatory device to control the excitability of neurons. AMPARs-mediated transmission in the hypothalamus was believed to orchestrate the influence of glutamatergic transmission in neuroendocrine function, autonomic nervous system activity, social behavior, and other aspects [43]. In our previous research, GABAARs were found to contribute to the modulation of visceral hypersensitivity via the avBNST-PVN pathway [17, 28]. As expected, we further confirmed that an AMPAR antagonist and a GABAAR agonist reversed visceral pain-related behaviors in vivo (Supplementary Fig. S7). However, NMDAR- and GABAR- dependent plasticity in the anteromedial and anterolateral parts of the BNST is instrumental for anxiolysis and HPA axis activity [44, 45]. Thus, we cannot rule out the possibility that MS-induced susceptibility to visceral hypersensitivity may be due in part to activation of other subregions of the BNST, resulting in sensitivity to the HPA axis. In addition, in combination with neural activation, anatomical limitations and the density of distribution upstream, we also assessed the role of VMH-PVN and NAc-PVN neurocircuitry in visceral hypersensitivity (Supplementary Fig. S8). We observed that inhibition of VMH/NAc terminals in the PVN had no effect on visceral hypersensitivity in the susceptible group. It is presumed that the murine ventromedial hypothalamus is mainly composed of the VMH, MPA and Arc, which are highly conserved areas involved in behavior (including feeding and aggression), obesity, and homeostasis [46–48], etc. NAc is considered to mediate feeding, motivation, addiction, awakening, emotion and brain reward system [49–51], etc. Overall, our circuit and behavioral results showed that PVN CRH neurons of susceptible mice modulate visceral pain at least partially in response to projections from the avBNST.

According to the theory of sensitization and the cumulative stress hypothesis, ELS results in a continuous state of sensitivity to stress, which aids in the development of adaptive personality traits [52]. Some individuals exposed to ELS display psychological and behavioral resilience, which is associated with alterations in structure, function, and connectivity in the brain [53]. The mismatch hypothesis emphasizes the interplay between ELS and later-life stressors [54]. In our MS model, susceptible and resilient individuals could be distinguished as adults in the resting stage without stressor exposure. The PVN CRH neurons in resilient mice showed a "blunted" ability to induce compensatory changes in the context of increased excitatory postsynaptic efficiency. Importantly, calcium-activated potassium channels, through which intracellular calcium is associated with excitability, are responsible for many cellular processes, such as the control of neuronal intrinsic firing patterns, regulation of neurotransmission and manipulation of pain sensation [55, 56]. As nonvoltage-dependent Ca^{2+}-activated K^+ channels, SK2 channels can regulate the firing frequency of neurons by giving rise to I_{AHP} carried by K^+ [57, 58]. Our previous studies also demonstrated that decreased SK2 channel activity and protein expression in PVN or spinal dorsal horn neurons is associated with the occurrence of visceral hypersensitivity [30, 59, 60]. In this study, we observed the resilient mice show increased SK2 channel conductance in PVN CRH neurons which decreased CRH neural activation. Prospectively, the theory of visceral hypersensitivity resilience is still nascent and there is scope for a lot of new insights to be included in it.

In conclusion, we provide evidence that neuronal excitation in the avBNST modulates the activity of CRH neurons in the PVN in mice susceptible to visceral hypersensitivity and that SK2 expression and activity in PVN are associated with alleviated visceral hypersensitivity and pain (Supplementary Fig. S9). Overwhelming activation of the glutamatergic avBNST-PVN pathway or disinhibition of the GABAergic avBNST-PVN pathway has been found to predispose mice to MS-induced visceral hypersensitivity, and targeting glutamatergic or GABAergic receptors may be used to promote avBNST-PVN circuit activity for the treatment of visceral hypersensitivity. Moreover, deep brain stimulation (DBS) of the BNST has been utilized in the clinical treatment of psychosocial disorders [61]. Our present findings identify the potential neurocircuitry involved in chronic visceral pain and provide a molecular basis for the treatment of this condition.

REFERENCES

1. Prusator DK, Andrews A, Greenwood-Van Meerveld B. Neurobiology of early life stress and visceral pain: translational relevance from animal models to patient care. Neurogastroenterol Motil. 2016;28:1290–305.
2. de Maat DA, Schuurmans IK, Jongerling J, Metcalf SA, Lucassen N, Franken IHA, et al. Early life stress and behavior problems in early childhood: investigating the

contributions of child temperament and executive functions to resilience. Child Dev. 2022;93:e1–e16.
3. Farmer AD, Aziz Q. Gut pain & visceral hypersensitivity. Br J Pain. 2013;7:39–47.
4. Tang HL, Zhang G, Ji NN, Du L, Chen BB, Hua R, et al. Toll-like receptor 4 in paraventricular nucleus mediates visceral hypersensitivity induced by maternal separation. Front Pharm. 2017;8:309.
5. Colmers PLW, Bains JS. Balancing tonic and phasic inhibition in hypothalamic corticotropin-releasing hormone neurons. J Physiol. 2018;596:1919–29.
6. Lu J, Li Q, Xu D, Liao Y, Wang H. Programming of a developmental imbalance in hypothalamic glutamatergic/GABAergic afferents mediates low basal activity of the hypothalamic-pituitary-adrenal axis induced by prenatal dexamethasone exposure in male offspring rats. Toxicol Lett. 2020;331:33–41.
7. Banihashemi L, Sheu LK, Midei AJ, Gianaros PJ. Childhood physical abuse predicts stressor-evoked activity within central visceral control regions. Soc Cogn Affect Neurosci. 2015;10:474–85.
8. Banihashemi L, O'Neill EJ, Rinaman L. Central neural responses to restraint stress are altered in rats with an early life history of repeated brief maternal separation. Neuroscience. 2011;192:413–28.
9. Xiao Q, Zhou X, Wei P, Xie L, Han Y, Wang J, et al. A new GABAergic somatostatin projection from the BNST onto accumbal parvalbumin neurons controls anxiety. Mol Psychiatry. 2020;26:4719–41.
10. Salimando GJ, Hyun M, Boyt KM, Winder DG. BNST GluN2D-containing NMDA receptors influence anxiety- and depressive-like behaviors and modulatecell-specific excitatory/inhibitory synaptic balance. J Neurosci. 2020;40:3949–68.
11. Kasten CR, Carzoli KL, Sharfman NM, Henderson T, Holmgren EB, Lerner MR, et al. Adolescent alcohol exposure produces sex differences in negative affect-like behavior and group I mGluR BNST plasticity. Neuropsychopharmacology. 2020;45:1306–15.
12. Elharrar E, Warhaftig G, Issler O, Sztainberg Y, Dikshtein Y, Zahut R, et al. Overexpression of corticotropin-releasing factor receptor type 2 in the bed nucleus of stria terminalis improves posttraumatic stress disorder-like symptoms in a model of incubation of fear. Biol Psychiatry. 2013;74:827–36.
13. Song SY, Zhai XM, Dai JH, Lu LL, Shan CJ, Hong J, et al. Novel projections to the cerebrospinal fluid-contacting nucleus from the subcortex and limbic system in rat. Front Neuroanat. 2020;14:57.
14. Halladay LR, Herron SM. Lasting impact of postnatal maternal separation on the developing BNST: lifelong socioemotional consequences. Neuropharmacology. 2023;225:109404.
15. Banihashemi L, Peng CW, Rangarajan A, Karim HT, Wallace ML, Sibbach BM, et al. Childhood threat is associated with lower resting-state connectivity within a central visceral network. Front Psychol. 2022;13:805049.
16. Sawchenko PE, Swanson LW. The organization of forebrain afferents to the paraventricular and supraoptic nuclei of the rat. J Comp Neurol. 1983;218:121–44.
17. Song Y, Meng QX, Wu K, Hua R, Song ZJ, Song Y, et al. Disinhibition of PVN-projecting GABAergic neurons in AV region in BNST participates in visceral hypersensitivity in rats. Psychoneuroendocrinology. 2020;117:104690.
18. Cullinan WE, Herman JP, Watson SJ. Ventral subicular interaction with the hypothalamic paraventricular nucleus: evidence for a relay in the bed nucleus of the stria terminalis. J Comp Neurol. 1993;332:1–20.
19. Kudo T, Uchigashima M, Miyazaki T, Konno K, Yamasaki M, Yanagawa Y, et al. Three types of neurochemical projection from the bed nucleus of the stria terminalis to the ventral tegmental area in adult mice. J Neurosci. 2012;32:18035–46.
20. Poulin JF, Arbour D, Laforest S, Drolet G. Neuroanatomical characterization of endogenous opioids in the bed nucleus of the stria terminalis. Prog Neuropsychopharmacol Biol Psychiatry. 2009;33:1356–65.
21. Radley JJ, Gosselink KL, Sawchenko PE. A discrete GABAergic relay mediates medial prefrontal cortical inhibition of the neuroendocrine stress response. J Neurosci. 2009;29:7330–40.
22. Radley JJ, Sawchenko PE. A common substrate for prefrontal and hippocampal inhibition of the neuroendocrine stress response. J Neurosci. 2011;31:9683–95.
23. Choi DC, Furay AR, Evanson NK, Ostrander MM, Ulrich-Lai YM, Herman JP. Bed nucleus of the stria terminalis subregions differentially regulate hypothalamic-pituitary-adrenal axis activity: implications for the integration of limbic inputs. J Neurosci. 2007;27:2025–34.
24. Johnson SB, Emmons EB, Anderson RM, Glanz RM, Romig-Martin SA, Narayanan NS, et al. A basal forebrain site coordinates the modulation of endocrine and behavioral stress responses via divergent neural pathways. J Neurosci. 2016;36:8687–99.
25. Hiscox LV, Bray S, Fraser A, Meiser-Stedman R, Seedat S, Halligan SL. Sex differences in the severity and natural recovery of child PTSD symptoms: a longitudinal analysis of children exposed to acute trauma. Psychol Med. 2023;53:2682–8.
26. Giacometti LL, Huh JW, Raghupathi R. Sex and estrous-phase dependent alterations in depression-like behavior following mild traumatic brain injury in adolescent rats. J Neurosci Res. 2022;100:490–505.
27. Own LS, Iqbal R, Patel PD. Maternal separation alters serotonergic and HPA axis gene expression independent of separation duration in mice. Brain Res. 2013;1515:29–38.
28. Huang ST, Song ZJ, Liu Y, Luo WC, Yin Q, Zhang YM. BNST(AV) (GABA)-PVN(CRF) circuit regulates visceral hypersensitivity induced by maternal separation in Vgat-Cre mice. Front Pharm. 2021;12:615202.
29. Wickersham IR, Lyon DC, Barnard RJ, Mori T, Finke S, Conzelmann KK, et al. Monosynaptic restriction of transsynaptic tracing from single, genetically targeted neurons. Neuron. 2007;53:639–47.
30. Ji NN, Du L, Wang Y, Wu K, Chen ZY, Hua R, et al. Small-conductance Ca(2+)-activated K(+) channels 2 in the hypothalamic paraventricular nucleus precipitates visceral hypersensitivity induced by neonatal colorectal distension in rats. Front Pharm. 2020;11:605618.
31. Orso R, Creutzberg KC, Wearick-Silva LE, Wendt Viola T, Tractenberg SG, Benetti F, et al. How early life stress impact maternal care: a systematic review of rodent studies. Front Behav Neurosci. 2019;13:197.
32. Fisher H, Morgan C, Dazzan P, Craig TK, Morgan K, Hutchinson G, et al. Gender differences in the association between childhood abuse and psychosis. Br J Psychiatry. 2009;194:319–25.
33. Anbardan SJ, Daryani NE, Fereshtehnejad SM, Taba Taba Vakili S, Keramati MR, Ajdarkosh H. Gender role in irritable bowel syndrome: a comparison of irritable bowel syndrome module (ROME III) between male and female patients. J Neurogastroenterol Motil. 2012;18:70–7.
34. Herzberg MP, Gunnar MR. Early life stress and brain function: activity and connectivity associated with processing emotion and reward. Neuroimage. 2020;209:116493.
35. Louwies T, Mohammadi E, Greenwood-Van, Meerveld B. Epigenetic mechanisms underlying stress-induced visceral pain: resilience versus vulnerability in a two-hit model of early life stress and chronic adult stress. Neurogastroenterol Motil. 2023;35:e14558.
36. Prusator DK, Greenwood-Van, Meerveld B. Gender specific effects of neonatal limited nesting on viscerosomatic sensitivity and anxiety-like behavior in adult rats. Neurogastroenterol Motil. 2015;27:72–81.
37. Fuentes IM, Christianson JA. The influence of early life experience on visceral pain. Front Syst Neurosci. 2018;12:2.
38. Gunn BG, Cunningham L, Cooper MA, Corteen NL, Seifi M, Swinny JD, et al. Dysfunctional astrocytic and synaptic regulation of hypothalamic glutamatergic transmission in a mouse model of early-life adversity: relevance to neurosteroids and programming of the stress response. J Neurosci. 2013; 33:19534–54.
39. Cullinan WE, Ziegler DR, Herman JP. Functional role of local GABAergic influences on the HPA axis. Brain Struct Funct. 2008;213:63–72.
40. Emmons R, Sadok T, Rovero NG, Belnap MA, Henderson HJM, Quan AJ, et al. Chemogenetic manipulation of the bed nucleus of the stria terminalis counteracts social behavioral deficits induced by early life stress in C57BL/6J mice. J Neurosci Res. 2021;99:90–109.
41. Jennings JH, Sparta DR, Stamatakis AM, Ung RL, Pleil KE, Kash TL, et al. Distinct extended amygdala circuits for divergent motivational states. Nature. 2013;496:224–8.
42. Gungor NZ, Yamamoto R, Pare D. Glutamatergic and gabaergic ventral BNST neurons differ in their physiological properties and responsiveness to noradrenaline. Neuropsychopharmacology. 2018;43:2126–33.
43. Royo M, Escolano BA, Madrigal MP, Jurado S. AMPA receptor function in hypothalamic synapses. Front Synaptic Neurosci. 2022;14:833449.
44. Glangetas C, Massi L, Fois GR, Jalabert M, Girard D, Diana M, et al. NMDA-receptor-dependent plasticity in the bed nucleus of the stria terminalis triggers long-term anxiolysis. Nat Commun. 2017;8:14456.
45. Gafford GM, Ressler KJ. GABA and NMDA receptors in CRF neurons have opposing effects in fear acquisition and anxiety in central amygdala vs. bed nucleus of the stria terminalis. Horm Behav. 2015;76:136–42.
46. McClellan KM, Parker KL, Tobet S. Development of the ventromedial nucleus of the hypothalamus. Front Neuroendocrinol. 2006;27:193–209.
47. Karigo T, Kennedy A, Yang B, Liu M, Tai D, Wahle IA, et al. Distinct hypothalamic control of same- and opposite-sex mounting behaviour in mice. Nature. 2021;589:258–63.
48. Todd WD, Fenselau H, Wang JL, Zhang R, Machado NL, Venner A, et al. A hypothalamic circuit for the circadian control of aggression. Nat Neurosci. 2018;21:717–24.
49. Jiang K, Xue P, Xu Y, Yi Y, Zhu J, Ding L, et al. The brain mechanism of awakening dysfunction in children with primary nocturnal enuresis based on PVT-NAc neural pathway: a resting-state fMRI study. Sci Rep. 2021;11:17079.
50. Jiang C, Yang X, He G, Wang F, Wang Z, Xu W, et al. CRH(CeA–>VTA) inputs inhibit the positive ensembles to induce negative effect of opiate withdrawal. Mol Psychiatry. 2021;26:6170–86.

51. Sorinas J, Grima MD, Ferrandez JM, Fernandez E. Identifying suitable brain regions and trial size segmentation for positive/negative emotion recognition. Int J Neural Syst. 2019;29:1850044.
52. Mittal C, Griskevicius V, Simpson JA, Sung S, Young ES. Cognitive adaptations to stressful environments: when childhood adversity enhances adult executive function. J Pers Soc Psychol. 2015;109:604–21.
53. Eaton S, Cornwell H, Hamilton-Giachritsis C, Fairchild G. Resilience and young people's brain structure, function and connectivity: a systematic review. Neurosci Biobehav Rev. 2022;132:936–56.
54. Daskalakis NP, Oitzl MS, Schächinger H, Champagne DL, de Kloet ER. Testing the cumulative stress and mismatch hypotheses of psychopathology in a rat model of early-life adversity. Physiol Behav. 2012;106:707–21.
55. Berkefeld H, Fakler B, Schulte U. Ca2+-activated K+ channels: from protein complexes to function. Physiol Rev. 2010;90:1437–59.
56. Bahia PK, Suzuki R, Benton DC, Jowett AJ, Chen MX, Trezise DJ, et al. A functional role for small-conductance calcium-activated potassium channels in sensory pathways including nociceptive processes. J Neurosci. 2005;25:3489–98.
57. Thompson JM, Ji G, Neugebauer V. Small-conductance calcium-activated potassium (SK) channels in the amygdala mediate pain-inhibiting effects of clinically available riluzole in a rat model of arthritis pain. Mol Pain. 2015;11:51.
58. Honrath B, Krabbendam IE, Culmsee C, Dolga AM. Small conductance Ca(2+)-activated K(+) channels in the plasma membrane, mitochondria and the ER: pharmacology and implications in neuronal diseases. Neurochem Int. 2017;109:13–23.
59. Song Y, Zhu JS, Hua R, Du L, Huang ST, Stackman RW Jr, et al. Small-conductance Ca(2+)-activated K(+) channel 2 in the dorsal horn of spinal cord participates in visceral hypersensitivity in rats. Front Pharm. 2018;9:840.
60. Wu K, Gao JH, Hua R, Peng XH, Wang H, Zhang YM. Predisposition of neonatal maternal separation to visceral hypersensitivity via downregulation of small-conductance calcium-activated potassium channel subtype 2 (SK2) in mice. Neural Plast. 2020;2020:8876230.
61. Winter L, Saryyeva A, Schwabe K, Heissler HE, Runge J, Alam M, et al. Long-term deep brain stimulation in treatment-resistant obsessive-compulsive disorder: outcome and quality of life at four to eight years follow-up. Neuromodulation. 2020;24:324–30.

AUTHOR CONTRIBUTIONS

Conceptualization: STH, YMZ. Methodology and Investigation: STH, KW, MMG, SS. Supervision: RH, YMZ. Funding acquisition: STH, YMZ. Writing-original draft: STH, YMZ. Writing-revies & editing: STH, KW, MMG, SS, RH, YMZ.

FUNDING

The present study was supported by STI2030-Major Projects (2021ZD0203100), the National Natural Science Foundation of China (Grant Numbers 82271257, 82071228), and Startup Funds from Xuzhou Medical University (RC20552252).

COMPETING INTERESTS

The authors declare no competing interests.

ADDITIONAL INFORMATION

Supplementary information The online version contains supplementary material available at https://doi.org/10.1038/s41386-023-01678-1.

Correspondence and requests for materials should be addressed to Yong-Mei Zhang.

Reprints and permission information is available at http://www.nature.com/reprints

Publisher's note Springer Nature remains neutral with regard to jurisdictional claims in published maps and institutional affiliations.

Springer Nature or its licensor (e.g. a society or other partner) holds exclusive rights to this article under a publishing agreement with the author(s) or other rightsholder(s); author self-archiving of the accepted manuscript version of this article is solely governed by the terms of such publishing agreement and applicable law.